Motional effects of trapped atomic or ionic qubits

L. You
School of Physics, Georgia Institute of Technology, Atlanta, Georgia 30332-0430
(Received 14 August 2000; published 30 May 2001)

We investigate decoherence effects due to motional degrees of freedom of trapped electronically coded atomic or ionic qubits. For universal single bit rotations implemented with dipole coupling from a near resonant running wave laser, the achievable fidelity is found to depend only on a single parameter characterized by the initial motional state. For two-qubit conditional logic operations inside a high Q optical cavity, we find the popular dark state structure survives even when atomic wave packets are not localized along transverse directions. Our quantitative results provide a useful realistic view for current experimental efforts in quantum logic and computing.

DOI: 10.1103/PhysRevA.64.012302 PACS number(s): 03.67.Lx, 32.80.Pj, 42.50.Dv, 89.70.+c

I. INTRODUCTION

Since the pioneering work of Shor [1] on efficient prime factorization with a quantum computer in 1994, we have witnessed an explosive growth of interest in quantum information and computing. Although still largely a theoretical field, solid progress in experimental efforts have been made within the last few years. Most notably, success of pure state based quantum gate implementations [2], demonstrations of quantum teleportations [3], and GHZ state synthesis [4] have stimulated more vigorous experimental efforts.

The Innsbruck group suggested two of the most interesting proposals for potentially large scale quantum computing, based, respectively, on trapped ions [5] and cavity QED with atoms [6]. Many experiments around the world are actively pursuing the implementation of these ideas in various ways. In their original analysis as presented in Refs. [5,6], individual qubits are coded in electronic states of atoms or ions, and coherent evolution of the system requires all qubits to be in a particular (usually the ground) motional state. Experimentally, one needs to attain the strong binding limit [7] and cool atoms or ions to the motional ground state in all three dimensions [8]. It is well known that these limits are difficult to maintain due to various decoherence and dissipation processes [9], which may also heat up motional states. Furthermore, maintaining the motional ground state becomes problematic when strong confinement is not satisfied. Several ideas for computing with ''hot'' qubits were proposed recently to counter decoherence due to motional degrees of freedom [10].

Attempting to provide answers to motional effects (ME) on electronically encoded quantum states [11], this paper is the first step towards a thorough investigation of ME [12] in the universal quantum computing model based on trapped atoms inside a high Q optical cavity. This paper is organized as follows: first we discuss ME in universal unitary evolutions for single trapped qubits (two level atoms or ions) implemented through a resonant running wave laser. We will present the model and introduce a convenient and physical wave-packet basis for discussing analytically the decoherence ME of any (unknown) electronic encoded qubit. Second, we discuss the more complicated gate operations involving conditional dynamics of two interacting qubits through a single cavity photon [6]. We will present numerical results and analytical based analysis. Finally, we conclude.

II. A SINGLE TRAPPED QUBIT

Our model consists of a single harmonically trapped two state atom or ion described by the Hamiltonian [13–15]

$$H^{[1]}=H_{\mathrm{ME}}^{[1]}+H_{\mathrm{int}}^{[1]}, \tag{1}$$

$$H_{\mathrm{ME}}^{[1]}=\sum_{\vec{n}}\hbar(n_x\omega_x^g+n_y\omega_y^g+n_z\omega_z^g)|g,\vec{n}\rangle\langle g,\vec{n}| + \sum_{\vec{m}}\hbar(\omega_{eg}+m_x\omega_x^e+m_y\omega_y^e+m_z\omega_z^e)|e,\vec{m}\rangle\langle e,\vec{m}|, \tag{2}$$

$$H_{\mathrm{int}}^{[1]}=\frac{1}{2}\hbar\Omega_L e^{i\omega_L t}\sum_{\vec{n},\vec{m}}\eta_{\vec{n}\vec{m}}(\vec{k}_L)|g,\vec{n}\rangle\langle e,\vec{m}|+\mathrm{H.c.} \tag{3}$$

$|g,\vec{n}\rangle=|g\rangle|\vec{n}\rangle_g$ ($|e,\vec{m}\rangle=|e\rangle|\vec{m}\rangle_e$) denotes number state in the ground (excited) trap with frequencies $\omega_{i=x,y,z}^g(\omega_i^e)$. ω_{eg} is the electronic transition frequency. Ω_L is the Rabi frequency of the plane-wave laser field. The motional dipole moment is the familiar Franck-Condon factor [16]

$$\eta_{\vec{n}\vec{m}}(\vec{k}_L)=\langle g,\vec{n}|e^{-i\vec{k}_L\cdot\vec{R}}|e,\vec{m}\rangle. \tag{4}$$

Radiative coupling to the vacuum reservoir will not be included here as its effect on qubit decoherence has been extensively studied and is well understood [5,6,10,15,17,18]. This approximation can also be justified by regarding our two levels as between two ground states in a three level Λ-type off-resonant Raman system. In such a case, $\Omega_L \sim \Omega_P\Omega_S^*/\delta_L$ is the two photon effective Rabi frequency and $\vec{k}_L=\vec{k}_P-\vec{k}_S$. The indices P and S denote dipole connected pump and stokes transitions, and δ_L is the (large) detuning from the eliminated far off-resonant excited state. For logic operations involving electronic coded qubits, even a single

spontaneous emission event will wipe out the quantum coherence and prevent reliable quantum information processing.

Physical models similar to Eq. (3) have been studied extensively under different contexts [5,7,14,15,20,21]. In the so-called Lamb-Dicke limit (LDL) when an atom is confined to trap size $a_i^{g,e}=\sqrt{\hbar/2M\omega_i^{g,e}}$, satisfying $k_L a_i^{g,e}\ll 1$, ME considerably simplifies. The LDL is physically equivalent to requiring $\hbar\omega_i^g$ to be much larger than the recoil energy $E_R=\hbar^2k_L^2/2M\ll\hbar\omega_i^{e,g}$. For an effective two state system reduced from a near resonant three level Λ-type configuration, LDL is easily satisfied with co-propagating pump and Stokes fields when $\vec{k}_P\sim\vec{k}_S$. Beyond the LDL, ME becomes rather complicated. In their seminal study on the laser cooling of trapped particles, Wineland and Itano [18] have obtained results valid beyond LDL. More recently, effects beyond LDL were numerically studied by several other groups, including Zeng *et al.* [14] and Vogel and de Matos Filho [19].

In this paper we investigated ME for general electronically coded trapped qubits not necessarily in the LDL. Such theoretical studies are urgently needed as trapped atoms or ions are among the ''hottest'' qubit candidates in many experimental efforts. We aim at gaining physical insight into the detailed analytic structures of the coupling between plane-wave laser fields and harmonically trapped motional states. We note the motional dipole moment is the familiar Franck-Condon factor [22], which, in the notation of Ref. [16] is given by Eq. (4) satisfying

$$\sum_{\vec{n}} [\eta_{\vec{n}\vec{m}}(\vec{k}_L)]^*\eta_{\vec{n}\vec{m}'}(\vec{k}_L)=\delta_{\vec{m}\vec{m}'},$$
$$\sum_{\vec{m}} [\eta_{\vec{n}\vec{m}}(\vec{k}_L)]^*\eta_{\vec{n}'\vec{m}}(\vec{k}_L)=\delta_{\vec{n}\vec{n}'}. \tag{5}$$

This motivates the introduction of a complete and orthonormal basis

$$|\vec{n}^p\rangle_e=\sum_{\vec{n}'}\eta^*_{\vec{n}\vec{n}'}(\vec{k}_L)|\vec{n}'\rangle_e=e^{i\vec{k}_L\cdot\vec{R}}|\vec{n}\rangle_g. \tag{6}$$

Physically this basis corresponds to the motional wave packet after a photon absorption from ground motional state $|\vec{n}\rangle_g$. Mathematically, it is the number coherent state $|\alpha,n\rangle=D(\alpha)|n\rangle$, with the displacement operator $D(\alpha)=e^{\alpha b^\dagger-\alpha^* b}$ [23]. We note that $R_i=a_i^g(b_i^{g\dagger}+b_i^g)$ with b_i^g (b_i^{g+}) the annihilation (creation) operator for $|n_i\rangle_g$. Therefore Eq. (6) can be rewritten as $|n_x^p\rangle=|ik_La_x^g,n_x\rangle_g$ along the excitation direction. As will become clear later, the coherent Rabi coupling between the ground and excited-state manifolds can then be decomposed into paired sets $\{|g\rangle|\vec{n}\rangle_g,|e\rangle|\vec{n}^p\rangle_e\}$ with the same value of dipole coupling Ω_L. For trapped ions, $|\vec{n}\rangle_e=|\vec{n}\rangle_g$ as the confining potential is internal state independent (only depends on the charge distribution). One can then express $|\vec{n}^p\rangle_e$ in terms of a linear combination of motional state $|\vec{n}\rangle_g$ (or $|\vec{n}\rangle_e$) to arrive at a similar expression for the coupling term (3) as in Sec. 2.3.1 of Ref. [24].

The inverse relation of Eq. (6):

$$|\vec{m}\rangle_e=\sum_{\vec{n}}\eta_{\vec{n}\vec{m}}(\vec{k}_L)|\vec{n}^p\rangle_e, \tag{7}$$

allows us to transform the excited motional degrees of freedom of Eq. (2) into

$$\sum_{\vec{m}}\hbar\omega_{eg}|e,\vec{m}\rangle\langle e,\vec{m}|=\sum_{n}\hbar\omega_{eg}|e,\vec{n}^p\rangle\langle e,\vec{n}^p|,$$
$$\sum_{\vec{m},i}m_i\hbar\omega_i^e|\vec{m}\rangle_{ee}\langle\vec{m}|=\sum_{\vec{n}\vec{n}'}(E^D_{\vec{n}\vec{n}'}+E^O_{\vec{n}\vec{n}'})|\vec{n}^p\rangle_{ee}\langle\vec{n}'^p|. \tag{8}$$

We find $E^D_{\vec{n}\vec{n}'}$ terms couple nearest neighbors, i.e., states with $n_i=n_i'\pm 1$ ($n_{j\neq i}=n_j'$), while $E^O_{\vec{n}\vec{n}'}$ terms couple states with $\vec{n}=\vec{n}'$ and $n_i=n_i'\pm 2$ ($n_{j\neq i}=n_j'$).

We will focus on the case $\omega_i^g=\omega_i^e$ ($i=x,y,z$) in the present paper. This is typical for the ion traps and can also be arranged for optical dipole trapped atoms [25]. For plane-wave excitation along the x axis, the ME along the y and z directions are then unperturbed. Our Hamiltonian equation (3) simplifies to a one-dimensional model

$$\mathcal{H}^{[1]}=\mathcal{H}^{[1]}_{\rm ME}+\mathcal{H}^{[1]}_{\rm int}, \tag{9}$$

$$\mathcal{H}^{[1]}_{\rm ME}=\sum_{n_x}n_x\hbar\omega_x^g|g,n_x\rangle\langle g,n_x|+\sum_{n_x}\hbar(n_x\omega_x^g-\Delta_L)\times|e,n_x^p\rangle\langle e,n_x^p|+i(k_La_x)\sum_{n_x}\hbar\omega_x^g\sqrt{n_x+1}\times|e,n_x^p+1\rangle\langle e,n_x^p|+\text{H.c.}, \tag{10}$$

$$\mathcal{H}^{[1]}_{\rm int}=\frac{1}{2}\hbar\Omega_L\sum_{n_x}|g,n_x\rangle\langle e,n_x^p|+\text{H.c.}, \tag{11}$$

where transformation to the interaction picture by

$$U(t)=\exp\left(-i\hbar\omega_L t\sum_{n_x}|e,n_x^p\rangle\langle e,n_x^p|\right) \tag{12}$$

has also been made. The detuning is defined as $\hbar\Delta_L=\hbar\omega_L-\hbar\omega_{eg}-\hbar^2k_L^2/(2M)$, including recoil shift.

This Hamiltonian can be graphically illustrated as in Fig. 1. The paired ladder structure resembles the familiar LDL motional state ladders in an ion trap [7]. However, in this case as shown in Fig. 1, excited motional states are wave-packet states, Eq. (6). The nearest-neighbor coupling merely reflects Doppler effect in this wave-packet basis where kinetic-energy operator $-\hbar^2\nabla^2/(2M)$ transforms into $-\hbar^2(\nabla-ik_L)^2/(2M)$ Eq. (6). The term $i\hbar^2k_L\nabla/M$, linear in velocity $-i\hbar\nabla/M$, then couples nearest-neighbor wave-packet harmonic-oscillator states. Denoting $\mathcal{H}^{[1]}=\mathcal{H}^{[1]}_D$

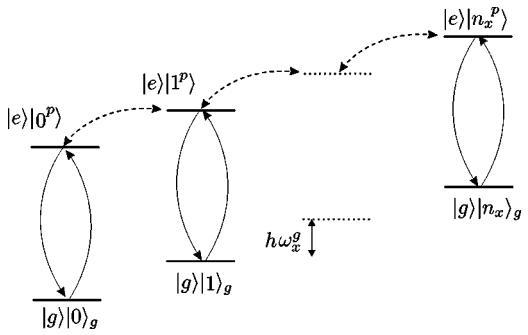

FIG. 1. The paired ladders of a trapped two state atom or ion. Solid curve arrow heads denote Rabi oscillations between paired states, while the dashed curve arrow heads denote nearest-neighbor motional coupling.

$+\mathcal{H}_O^{[1]}$ with $\mathcal{H}_O^{[1]}$ the nearest-neighbor coupling term in the excited state [the third line of Eq. (10)], $\mathcal{H}_D^{[1]}$ becomes

$$\mathcal{H}_D^{[1]}=\hbar\begin{pmatrix} \ddots & & & & \\ & n_x\omega_x^g & \frac{\Omega_L}{2} & & \\ & \frac{\Omega_L}{2} & n_x\omega_x^g-\Delta_L & & \\ & & & \ddots & \\ & & & & \end{pmatrix}, \quad (13)$$

where each 2×2 block describes the Rabi oscillation between paired states $\{|g\rangle|n_x\rangle_g, |e\rangle|n_x^p\rangle_e\}$ with *exactly the same* Rabi frequency $\Omega=\sqrt{\Omega_L^2+\Delta_L^2}$. There are no differential detunings between different pairs either. When on resonance $\Delta_L=0$, the wave function coefficients $\{c_{n_x}^g, c_{n_x}^e\}$ are easily solved to be

$$\begin{aligned} c_{n_x}^e(\tau)&=e^{-in_x\omega_x^g\tau}[c_{n_x}^e(0)\cos\theta-ic_{n_x}^g(0)\sin\theta],\\ c_{n_x}^g(\tau)&=e^{-in_x\omega_x^g\tau}[c_{n_x}^g(0)\cos\theta-ic_{n_x}^e(0)\sin\theta], \end{aligned} \quad (14)$$

with the pulse area defined as $\theta(\tau)=\frac{1}{2}\int_0^\tau\Omega(t)\,dt$. Thus, $\mathcal{H}_D^{[1]}$ describes a coherent evolution between paired states with a single time scale given by Ω. $\mathcal{H}_O^{[1]}$, on the other hand, can cause decoherence of an electronically coded qubit. It is due to the Doppler coupling that connects nearest neighbors (in a harmonic trap) of excited motional wavepack states. Its time scale is determined by several factors including the trap frequency ω_x^g, Lamb Dicke parameter $k_La_x^g$, and the highest motional state number $n_x^{\max}$. Assuming an electronically coded unknown qubit

$$|\psi(0)\rangle=\alpha|g\rangle+\beta|e\rangle \quad (15)$$

(normalization $|\alpha|^2+|\beta|^2=1$), an arbitrary single bit rotation is achieved through a multiplication of [26]

$$e^{i\delta}\begin{pmatrix} e^{i\gamma_1} & 0\\ 0 & e^{-i\gamma_1}\end{pmatrix}\begin{pmatrix}\cos\theta & \sin\theta\\ -\sin\theta & \cos\theta\end{pmatrix}\begin{pmatrix} e^{i\gamma_2} & 0\\ 0 & e^{-i\gamma_2}\end{pmatrix}$$

with parameters δ, γ_1, γ_2, and ϕ. For resonant Rabi coupling, our solution of Eq. (14) achieves the important θ rotation corresponding to $e^{2i\gamma_1}=-i$ and $e^{2i\gamma_2}=i$. Ideally one hopes to arrive at the target state

$$|\psi(\tau)\rangle_T=(\alpha\cos\theta-i\beta\sin\theta)|g\rangle+(\beta\cos\theta-i\alpha\sin\theta)|e\rangle,$$

with the density matrix

$$\rho_T(\tau)=I_g^T|g\rangle\langle g|+(1-I_g^T)|e\rangle\langle e|+(I_{ge}^T|g\rangle\langle e|+\text{H.c.}), \quad (16)$$

where

$$I_g^T=|\alpha|^2\cos^2\theta+|\beta|^2\sin^2\theta+i(\alpha\beta^*-\text{c.c.})\sin\theta\cos\theta,$$

$$I_{ge}^T=\alpha\beta^*\cos^2\theta+\beta\alpha^*\sin^2\theta+i(|\alpha|^2-|\beta|^2)\sin\theta\cos\theta.$$

Due to ME, the electronic qubit equation (15) does not remain decoupled from the motional degrees of freedom. Generally, it evolves within the much larger Hilbert space containing motional states. We now study two concrete examples of decoherence assuming the initial qubit in the enlarged Hilbert space reproduces the density matrix equation (16), i.e., resembles a perfect qubit to the innocent bystanders unaware of the motional degrees of freedom.

First, we consider

$$|\psi(0)\rangle_{\text{tot}}=(\alpha|g\rangle+\beta|e\rangle)\otimes|\psi(0)\rangle_{\text{cm}}, \quad (17)$$

with an initial pure motional state $|\psi(0)\rangle_{\text{cm}}=\Sigma_{n_x}c_{n_x}|n_x\rangle_g$ $(\Sigma_{n_x}|c_{n_x}|^2=1)$. Upon tracing the motional degrees of freedom, $\rho(0)=|\psi(0)\rangle\langle\psi(0)|$ is correctly reproduced. By rewriting $|\psi(0)\rangle_{\text{tot}}$ as

$$\sum_{n_x}\left(c_{n_x}\alpha|g\rangle|n_x\rangle_g+\sum_{n_x'}\eta_{n_xn_x'}c_{n_x'}\beta|e\rangle|n_x^p\rangle_e\right),$$

we can analytically evolve this state with $\mathcal{H}_D^{[1]}$ to obtain

$$\rho(\tau)=I_g|g\rangle\langle g|+(1-I_g)|e\rangle\langle e|+(I_{ge}|g\rangle\langle e|+\text{H.c.}), \quad (18)$$

with

$$I_g=|\alpha|^2\cos^2\theta+|\beta|^2\sin^2\theta+i(\alpha\beta^*\eta^*-\text{c.c.})\cos\theta\sin\theta,$$

$$I_{ge}=i(|\alpha|^2-|\beta|^2)\frac{1}{2}\sin 2\theta\sum_{n_x,q_x}\exp[-i(n_x-q_x)\omega_x^g\tau]\times c_{n_x}c_{q_x}^*\eta_{q_xn_x}+\alpha\beta^*\cos^2\theta\times\sum_{n_x,q_x}\exp[-i(n_x-q_x)\omega_x^g\tau]c_{n_x}\times\sum_{q_x'}\eta_{q_xq_x'}^*c_{q_x'}^*\eta_{q_xn_x}+\alpha^*\beta\sin^2\theta\times\sum_{n_x,q_x}\exp[-i(n_x-q_x)\omega_x^g\tau]\sum_{n_x'}\eta_{n_xn_x'}c_{n_x'}c_{q_x}^*\eta_{q_xn_x},$$

where we have defined the parameter

$$\eta(k_L)=\sum_{n_x,n_x'}c_{n_x}^*\eta_{n_xn_x'}c_{n_x'}. \tag{19}$$

We see the evolution given by Eq. (14) will in general not reproduce the intended density matrix equation (16) because η is not necessarily equal to unity. In addition, the effect of the $\mathcal{H}_O^{[1]}$ term causes the lack of complete control although its effects (when $\Omega_L\gg\omega_x^g$) can be minimized by employing faster pulses with $\omega_x^g\tau\ll 1$. Within such a limit, or when $\omega_x^g\tau=2\pi$, we obtain

$$I_{ge}=i(|\alpha|^2-|\beta|^2)\sin\theta\cos\theta\,\eta(k_L)+\alpha\beta^*\cos^2\theta+\alpha^*\beta\sin^2\theta\,\eta(2k_L). \tag{20}$$

The necessary condition for attending a perfect fidelity of the single bit rotation is then $\eta(k_L)\equiv 1$, which can be approximately satisfied in the LDL when $k_La_x^g\ll 1$, or in the Λ-type Raman systems with co-propagating pump and Stokes fields. As a second example, we consider the case of a thermal motional state

$$\rho_{\text{tot}}(0)=|\psi(0)\rangle\langle\psi(0)|\otimes\rho_{\text{cm}}(0),$$

$$\rho_{\text{cm}}(0)=\sum_{n_x}\rho_{n_x}^{\text{cm}}|n_x\rangle\langle n_x|,$$

$$\rho_{n_x}^{\text{cm}}=(1-\exp[-\hbar\omega_x^g/k_BT])\exp[-n_x\hbar\omega_x^g/k_BT]. \tag{21}$$

This is the limiting case of an ensemble average of Eq. (17) with $c_{n_x}=\sqrt{\rho_{n_x}^{\text{cm}}}e^{-i\phi_{n_x}}$ and ϕ_{n_x} a uniform random number $\in[0,2\pi)$. The dynamics due to $\mathcal{H}_D^{[1]}$ can again be evolved analytically and the same density matrix equation (18) is obtained. After averaging over $\{\phi_n\}$, we obtain

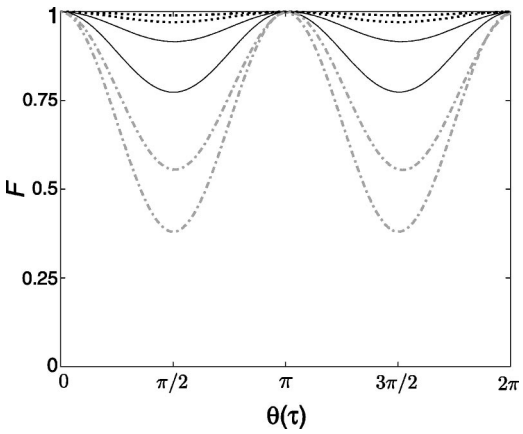

FIG. 2. The fidelity for single bit rotations with $k_La_x^g=0.1$ (dashed lines), 0.3 (solid lines), and 1.0 (dot dashed lines). The higher and lower fidelity sets are for initial motional state $c_{n_x}=\delta_{n_x0}$ and $c_{n_x}=(2\delta_{n_x0}+\sqrt{2}\,\delta_{n_x1}+\delta_{n_x2})/\sqrt{7}$, respectively. $\Omega_L=100(\omega_x^g)$.

$$\langle\eta(k_L)\rangle_{\{\phi_n\}}=\sum_{n_x}\rho_{n_x}^{\text{cm}}\eta_{n_xn_x}(k_L)=\exp\left[-\frac{1}{2}(k_La_x)^2\coth\left(\frac{1}{2}\frac{\hbar\omega_x^g}{k_BT}\right)\right]. \tag{22}$$

In the low-temperature limit, when $k_BT<\hbar\omega_x^g$, η becomes essentially indistinguishable from 1 as long as LDL $k_La_x^g\ll 1$ is satisfied. At high temperatures when $k_BT\gg\hbar\omega_x^g$, $(k_La_x^g)^2\ll\hbar\omega_x^g/k_BT$ needs to be satisfied for η to be close to unity. The latter condition is the same as $k_BT\ll(\hbar\omega_x^g)^2/E_R$.

We now discuss numerical solutions. We expand the total wave function as

$$|\psi(t)\rangle_{\text{tot}}=\sum_{n_x}[c_{n_x}^g(t)|g\rangle|n_x\rangle_g+c_{n_x}^e(t)|e\rangle|n_x^p\rangle_e], \tag{23}$$

and solve the Schrödinger equation including both $\mathcal{H}_D^{[1]}$ and $\mathcal{H}_O^{[1]}$. The transformation Eq. (6) greatly reduces the motional Hilbert-space dimension. The perceived fidelity for an electronically coded qubit equation (15) under transformation equation (16) is then

$$\mathcal{F}=\text{Tr}[\rho_T(\tau)\rho(\tau)]. \tag{24}$$

In the numerical results reported here, we take $\alpha=\beta=1/\sqrt{2}$ as an example. Similar or better fidelities were obtained with other unknown qubit choices. In Fig. 2 we compare fidelities under arbitrary $\theta(\tau)$ rotations for two different pure states. We see that acceptable fidelities are obtained only for $k_La_x^g\leqslant 0.3$. In general, larger Ω_L/ω_x^g ratios improve the maximum achievable fidelity although saturation is observed around $\Omega_L/\omega_x^g\sim 100$. This can be explained approximately with the illustrative level diagram in Fig. 1. At larger values of Ω_L, it takes less time to complete a given single qubit rotation (atomic Rabi oscillation). Thus motional decoherence is reduced due to the shortened duration for diffusive

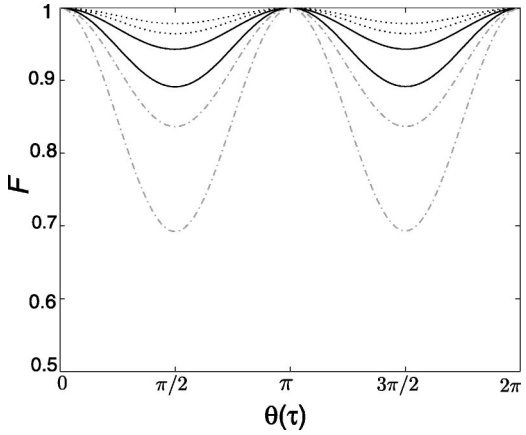

FIG. 3. The fidelity for single bit rotations with $k_BT/\hbar\omega_x^g=1$ (dashed lines), 3 (solid lines), and 10 (dot dashed lines). The higher and lower fidelity sets are for initial motional thermal state $\rho_{n_x}^{\rm cm}$ and pure state $c_{n_x}=\sqrt{\rho_{n_x}^{\rm cm}}$, respectively.

spreading of amplitudes in the excited-state manifold, resulting in a perceived improvement in fidelity. Noticeable improvements are also recorded for narrower initial distributions in $|c_n|^2$, e.g., in Fig. 2 the initial state with $c_{n_x}=\delta_{n_x0}$ produced the best fidelity. This is a direct reflection of dephasing among different motional pair states because of their different time scales from $\mathcal{H}_D^{[1]}$ and $\mathcal{H}_O^{[1]}$. The oscillatory behavior is caused by ME superposed on the synchronized Rabi oscillations among all motional state pairs. For comparison, we note that meaningful single bit rotations are only obtained for a fidelity $\geqslant 1/2$, the lower limit from a random (uncontrolled) sampling of final states.

Finally we study thermal motional states for several different values of $k_BT/\hbar\omega_x^g$. Surprisingly, we find fidelities for an initial motional thermal state is always higher than its corresponding pure state. This point deserves further investigation as we cannot provide an intuitive picture to aid understanding. In the temperature regime considered we find acceptable results as long as LDL is maintained. In Fig. 3, we show results for $k_La_x^g=0.1$ and $\Omega_L=100(\omega_x^g)$.

III. TWO INTERACTING QUBITS

We next consider the application of wave-packet transformation technique Eq. (6) to two interacting qubits. Our particular example involves two three-level Λ-type atoms trapped inside a high Q optical cavity as illustrated in Fig. 4 [6].

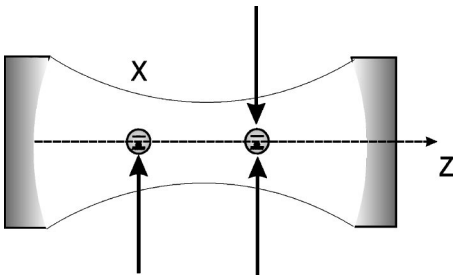

FIG. 4. The schematic for a cavity QED quantum gate implementation [6]. Solid lines denote coupling from running wave laser fields along the x-axis driving transition $|g_1\rangle\rightarrow|e\rangle$. The dashed line denotes cavity axis along z.

The cavity field mode function is described by

$$g(\vec{r})=g_0\frac{w_0}{w(z)}\exp\left[-\frac{\rho^2}{w^2(z)}\right]\sin(k_cz), \tag{25}$$

with $\rho^2=x^2+y^2$, the transverse (polar) coordinate measured from the cylindrically symmetric cavity axis along z. Both atoms are coupled to the same cavity photon field. $z_0=\pi w_0^2/\lambda_c$ is the Rayleigh range. With typical geometries, the mode waist $w(z)=w_0\sqrt{1+z^2/z_0^2}$ is much larger the wavelength λ_c, making LDL difficult to achieve along the x axis. Localization along the cavity axis is relatively easier as the standing wave fields readily provide periodic wells separated by $\lambda_c/2$. To investigate the problematic ME along the $\hat{x}$ direction, we therefore assume, in this paper, that an additional strong optical field (as recently implemented by Kimble *et al.* [27]) traps atoms into the motional ground state along the optical axis $\hat{z}$ in the LDL. Apart from other technical reasons, the illustration in Fig. 4 proves to be a convenient setup as control lasers directed along the transverse direction enable more flexibility in individual qubit addressing.

The simplified Hamiltonian for our model then becomes

$$H^{[2]}=H_{\rm ME}^{[2]}+H_{\rm int}^{[2]}+\hbar\omega_c a_c^\dagger a_c, \tag{26}$$

$$H_{\rm ME}^{[2]}=\sum_{\mu=A,B}\sum_{n_x}\sum_{j=1,2}\hbar n_x\omega_x^{g_j}(|g_j,n_x\rangle\langle g_j,n_x|)_\mu + \sum_{\mu=A,B}\sum_{m_x}(\hbar\omega_{eg}+\hbar m_x\omega_x^e)(|e,m_x\rangle\langle e,m_x|)_\mu, \tag{27}$$

$$H_{\rm int}^{[2]}=\frac{1}{2}\hbar\Omega_1^\mu e^{i\omega_1 t}\sum_{\mu=A,B}\sum_{n_x,m_x}\eta_{n_xm_x}^\mu(k_1)(|g_1,n_x\rangle\langle e,m_x|)_\mu + {\rm H.c.}+e^{i\omega_c t}a_c^\dagger\sum_{\mu=A,B}\hbar g_\mu\sum_{n_x}(|g_2,n_x\rangle\langle e,n_x|)_\mu + {\rm H.c.}, \tag{28}$$

where the remaining motional effect is along the harmonically confined x axis. The coupling with the cavity mode along this direction is taken as a constant $g_\mu=g_0(\vec{\rho}_\mu=0)$ by assuming harmonic atom traps to be centered on the z axis with trap size along x much smaller than $\omega(z)$. This model therefore allows for detailed investigations of the dominant ME effect along the exciting laser direction x. We emphasize that there are two separate motional states associated with each of atoms A and B, respectively. The trap frequencies for the two atoms are assumed the same to simplify notations, although this assumption is not needed to reach the same conclusion in the end.

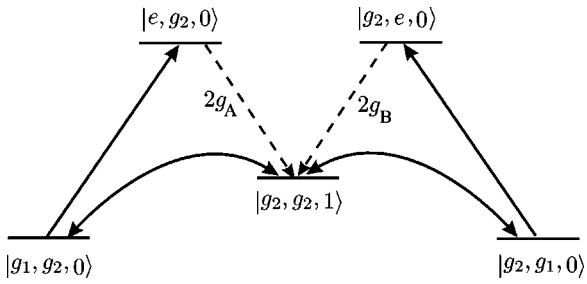

FIG. 5. Adiabatic passage energy-level diagram for the combined system of two Λ-type atoms plus a single mode cavity. Solid lines denote coupling from running wave laser fields connecting transition $|g_1\rangle \rightarrow |e\rangle$. The dashed lines are for couplings of the cavity photon with $|g_2\rangle \rightarrow |e\rangle$. The curved double headed arrows illustrate effective Raman coupling between $|g_1\rangle$ and $|g_2\rangle$ in the large detuning limit.

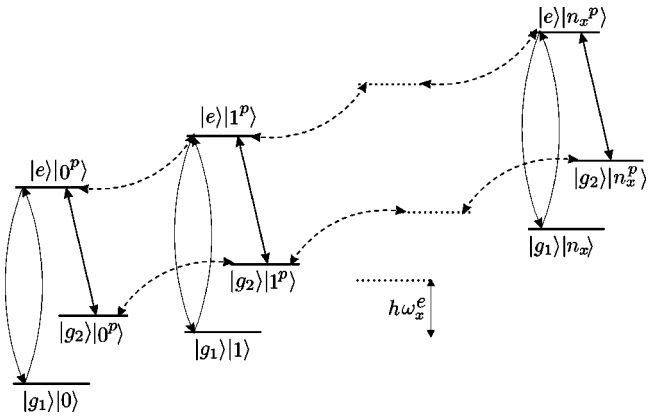

FIG. 6. The motional ladders of a trapped three level atom. Solid curve arrow heads denote Rabi oscillations between paired states, while the dotted curve arrow heads denote nearest-neighbor motional coupling. The straight arrow heads denote cavity mode coupling, which only connects states $|e,n_x^p\rangle$ with $|g_2,n_x^p\rangle$, i.e., states with the same motional wave packet because of the assumption that the trap size is much smaller than the cavity mode waist. Similar dark-state-like structures to Fig. 5 then arise involving a ladder of triplets for both atoms.

When LDL is also satisfied along the x axis and all atoms start in the ground state, the motional degrees of freedom become frozen, and a dark state exists for the composite atom plus cavity system [6]

$$|\mathrm{Dark}\rangle_1 = \frac{1}{2}\Omega_1^A\Omega_1^B|g_2,g_2,1\rangle - g_A\Omega_1^B|g_1,g_2,0\rangle - g_B\Omega_1^A|g_2,g_1,0\rangle, \tag{29}$$

as illustrated in Fig. 5 above. In the joint wave-function basis, we used the convention that the first index is for atom A, the second index is for a atom B, while the last one is for cavity photon number.

With time-dependent fields $\Omega_1^\mu(t)$, it is then possible to adiabatically change the state from $|g_1,g_2,0\rangle$ to $|g_2,g_1,0\rangle$ using counterintuitive pulse sequences with $\Omega_1^B(t)$ first on and $\Omega_1^A(t)$ last off. This operation is at the heart of universal quantum computing with an array of atoms inside an optical cavity [6]. The question we want to address now is, how will the ME along the x direction affect the above adiabatic transfer?

To simplify the analysis we further assume motional traps along x to be identical and independent of atomic internal states. We again take $\omega_x^e = \omega_x^{g_1} = \omega_x^{g_2} \equiv \omega_x^g$, although this is really not needed with the wave-packet basis approach [Eq. (6)] as we can show that our final conclusions are essentially independent of this assumption. The problem of two coupled atoms can then be studied by writing the total time-dependent wave function in the joint basis states $|\nu_A,\nu_B,n_c;n_x,m_x\rangle$, where $n_c = a_c^\dagger a_c$ is the cavity mode photon number. Using our wave-packet basis equation (6) for both the excited state $|e\rangle$ and final state $|g_2\rangle$, and transforming to the interaction picture with Eq. (12) for both atoms, we obtain

$$\mathcal{H}^{[2]} = \mathcal{H}_D^{[2]} + \mathcal{H}_{\mathrm{int}}^{[2]} + \mathcal{H}_O^{[2]}, \tag{30}$$

$$\mathcal{H}_D^{[2]} = \sum_{\mu=A,B}\sum_{n_x} n_x\hbar\omega_x^g(|g_1,n_x\rangle\langle g_1,n_x|)_\mu + \sum_{\mu=A,B}\sum_{m_x}(m_x\hbar\omega_x^g - \hbar\Delta_2)(|g_2,m_x^{\xi_\mu p}\rangle\langle g_2,m_x^{\xi_\mu p}|)_\mu + \sum_{\mu=A,B}\sum_{n_x}(n_x\hbar\omega_x^g - \hbar\Delta_1)(|e,n_x^{\xi_\mu p}\rangle\langle e,n_x^{\xi_\mu p}|)_\mu, \tag{31}$$

$$\mathcal{H}_{\mathrm{int}}^{[2]} = \frac{1}{2}\sum_{\mu=A,B}\sum_{n_x}\hbar\Omega_1^\mu(|g_1,n_x\rangle\langle e,n_x^{\xi_\mu p}|)_\mu + \mathrm{H.c.} + a_c^\dagger\sum_{\mu=A,B}\hbar g_\mu\sum_{n_x}(|g_2,n_x^{\xi_\mu p}\rangle\langle e,n_x^{\xi_\mu p}|)_\mu + \mathrm{H.c.}, \tag{32}$$

$$\mathcal{H}_O^{[2]} = i(k_1a_x^g)\sum_{\mu=A,B}\xi_\mu\sum_{n_x}\hbar\omega_x^g\sqrt{n_x+1}(|e,n_x^{\xi_\mu p}+1\rangle\times\langle e,n_x^{\xi_\mu p}|)_\mu + \mathrm{H.c.} + i(k_1a_x^g)\sum_{\mu=A,B}\xi_\mu\sum_{m_x}\hbar\omega_x^g\sqrt{m_x+1}(|g_2,m_x^{\xi_\mu p}+1\rangle\times\langle g_2,m_x^{\xi_\mu p}|)_\mu + \mathrm{H.c.}, \tag{33}$$

where $\hbar\Delta_1 = \hbar(\omega_1 - \omega_{eg_1}) - \hbar^2k_1^2/2M$, and $\hbar\Delta_2 = \hbar(\omega_1 - \omega_c - \omega_{g_2g_1}) - \hbar^2k_1^2/2M$ including recoil shift. $\xi_A = 1$ and $\xi_B = \pm 1$ denote directions of external laser fields. Physically, the laser field creates an excited motional state of atom A with a momentum kick $\hbar\vec{k}_L = \hbar\vec{k}_1$ along the positive x-axis direction. Atom B's excited motional wave-packet state,

however, can be moving into either positive ($\xi_B=1$) or negative ($\xi_B=-1$) directions depending on the direction of its stimulating laser. The single atom Hamiltonian graphically now becomes a ladder of Λ triplets as in Fig. 6.

Solutions to these Hamiltonians (31), (32), and (33) can be consistently classified within the resonant excitation approximation (neglecting counter rotating wave terms). In fact, solutions in blocks labeled by $|g_2,g_2,n_c;n_x,m_x\rangle$ with different n_c, do not couple to each other. In particular, when $n_c=0$, any motional state superposition in (n_x,m_x) of $|g_2,g_2,0;n_x,m_x\rangle$ remains an eigenstate of $\mathcal{H}_D^{[2]}$. Of particular interest is the fact that such states do not couple to any state with excitations e_A, e_B, or $n_c>0$. This is the family of dark states $|g_2,g_2,0\rangle$. When $n_c=1$, only 5 different types of states are coupled together by $\mathcal{H}_{\rm int}^{[2]}$, which allows us to write

$$
\begin{aligned}
|\Psi(t)\rangle_1=&\sum_{n_x,m_x} c_{g_1,g_2;n_x,m_x}(t)|g_1,g_2,0;n_x,m_x^{\xi_B p}\rangle\\
&+\sum_{n_x,m_x} c_{e,g_2;n_x,m_x}(t)|e,g_2,0;n_x^p,m_x^{\xi_B p}\rangle\\
&+\sum_{n_x,m_x} c_{g_2,g_2;n_x,m_x}(t)|g_2,g_2,1;n_x^p,m_x^{\xi_B p}\rangle\\
&+\sum_{n_x,m_x} c_{g_2,e;n_x,m_x}(t)|g_2,e,0;n_x^p,m_x^{\xi_B p}\rangle\\
&+\sum_{n_x,m_x} c_{g_2,g_1;n_x,m_x}(t)|g_2,g_1,0;n_x^p,m_x\rangle, \quad (34)
\end{aligned}
$$

where the wave-packet basis notation has been adopted. Not surprisingly, the dark-state-like structure Eq. (29) still exists; now between two atoms in any pair of triplet motional states $(|g_1\rangle|n_x\rangle,|e\rangle|n_x^p\rangle_e,|g_2\rangle|n_x^p\rangle_{g_2})$ for atom A and $(|g_1\rangle|m_x\rangle,|e\rangle|m_x^{\xi_\mu p}\rangle_e,|g_2\rangle|m_x^{\xi_\mu p}\rangle_{g_2})$ for atom B. This particular structure survives in such a transparent form due to the simplification of the wave-packet basis.

We now study how the ME affects the efficiency of the adiabatic state swap $|g_1,g_2,0\rangle\rightarrow|g_2,g_1,0\rangle$ using counterintuitive pulse sequences. We note

$$
\begin{aligned}
&\mathcal{H}_{\rm int}^{[2]}|\Psi(t)\rangle_1\\
&=\sum_{n_x,m_x}\left\{\left[\frac{1}{2}\hbar\Omega_1^A c_{g_1,g_2;n_x,m_x}(t)\right.\right.\\
&\quad\left.+\hbar g_A c_{g_2,g_2;n_x,m_x}(t)\right]|e,g_2,0;n_x^p,m_x^{\xi_B p}\rangle.\\
&\quad+\left[\frac{1}{2}\hbar\Omega_1^B c_{g_2,g_1;n_x,m_x}(t)+\hbar g_B c_{g_2,g_2;n_x,m_x}(t)\right]\\
&\quad\times|g_2,e,0;n_x^p,m_x^{\xi_B p}\rangle\Big\}\\
&\quad+\sum_{n_x,m_x}\left\{\frac{1}{2}\hbar\Omega_1^A c_{e,g_2;n_x,m_x}(t)|g_1,g_2,0;n_x,m_x^{\xi_B p}\rangle\right.\\
&\quad\left.+\frac{1}{2}\hbar\Omega_1^B c_{g_2,e;n_x,m_x}(t)|g_2,g_1,0;n_x^p,m_x\rangle\right\}\\
&\quad+\sum_{n_x,m_x}[\hbar g_A c_{e,g_2;n_x,m_x}(t)\\
&\quad+\hbar g_B c_{g_2,e;n_x,m_x}(t)]|g_2,g_2,1;n_x^p,m_x^{\xi_B p}\rangle, \quad (35)
\end{aligned}
$$

become identically zero for

$$
\begin{aligned}
&c_{g_1,g_2;n_x,m_x}(t)=-g_A\Omega_1^B(t),\\
&c_{e,g_2;n_x,m_x}(t)=0,\\
&c_{g_2,g_2;n_x,m_x}(t)=\frac{1}{2}\Omega_1^A(t)\Omega_1^B(t),\\
&c_{g_2,e;n_x,m_x}(t)=0,\\
&c_{g_2,g_1;n_x,m_x}(t)=-g_B\Omega_1^A(t). \quad (36)
\end{aligned}
$$

This is precisely the dark state condition Eq. (29), now generalized among all motional state triplets discussed earlier.

Our numerical procedure starts with an initial two atom motional wave function

$$
|\Psi(0)\rangle=|g_1,g_2,0\rangle\otimes|\psi\rangle_A\otimes|\psi\rangle_B, \quad (37)
$$

composed of separable identical single atom motional states

$$
|\psi\rangle_\mu=\sum_{n_x} c_{n_x}(0)|n_x\rangle_\mu. \quad (38)
$$

If all off-diagonal coupling terms $\mathcal{H}_{\rm ME}^{[2]O}$ and $\mathcal{H}_{\rm ME}^{[2]O}$ were absent, perfect state swapping would be achieved because of the dark-state-like structure [Eq. (35)]. Under counterintuitively ordered pulses, the wave-function adiabatic follows the steps leading to

$$
\begin{aligned}
&|g_1,g_2,0\rangle\otimes|\psi\rangle_A\otimes|\psi\rangle_B\\
&=|g_1,g_2,0\rangle\otimes\sum_{n_x} c_{n_x}^A(0)|n_x\rangle\\
&\quad\otimes\sum_{m_x}\sum_{l_x} c_{m_x}^B(0)\,\eta_{l_x m_x}(\xi_B k_1)|l_x^{\xi_B p}\rangle\\
&\rightarrow|g_2,g_1,0\rangle\\
&\quad\otimes\sum_{n_x} c_{n_x}^A(0)|n_x^p\rangle\sum_{m_x}\sum_{l_x} c_{m_x}^B(0)\,\eta_{m_x l_x}^*(-\xi_B k_1)|l_x\rangle\\
&=|g_2,g_1,0\rangle\otimes\sum_{n_x} c_{n_x}^A(0)|n_x^p\rangle\otimes\sum_{m_x} c_{m_x}^B(0)|m_x^{-\xi_B p}\rangle\\
&=|g_2,g_1,0\rangle\otimes e^{ik_1 x_A}|\psi\rangle_A\otimes e^{-\xi_B ik_1 x_B}|\psi\rangle_B. \quad (39)
\end{aligned}
$$

The final-state motional wave packets are in fact changed with atom A's modified by the photon recoil $e^{ik_1x_A}$ due to absorption and atom B's modified by $e^{-\xi_B ik_1x_B}$ from stimu-

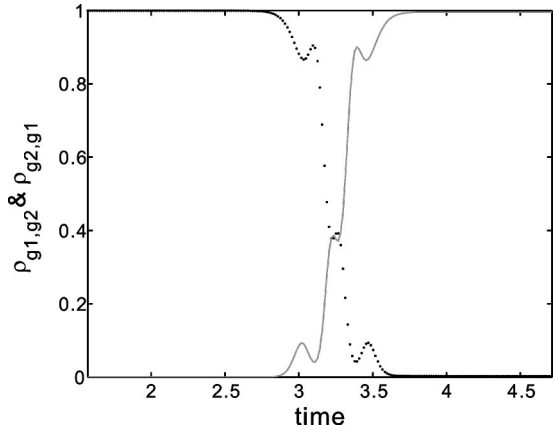

FIG. 7. The time-dependent probability of being in state $|g_1,g_2,0\rangle$ (dashed line) and $|g_2,g_1,0\rangle$ (solid line). A perfect fidelity $\mathcal{F}=\rho_{g2,g1}(t=2\pi)=1$ is essentially achieved in this case. $\rho_{\mu,\nu}$ is defined as $\Sigma_{n_x,m_x}|c_{\mu,\nu,0;n_x,m_x^p}|^2$.

lated emission into its driving laser field [28]. The two atom wave packets will therefore start moving in opposite directions for co-propagating control laser fields while going in the same direction for counterpropagating laser fields. However, this change of the motional state is a coherent process and becomes essentially transparent in our wave-packet basis. It does not lead to decoherence of quantum information coded in electronic qubits. The essential feature of the dark-state-like structure among any pairs of motional triplet ladder as given in Eq. (35) also enforces separable final motional states for atoms *A* and *B*. Consequently, we expect two-qubit

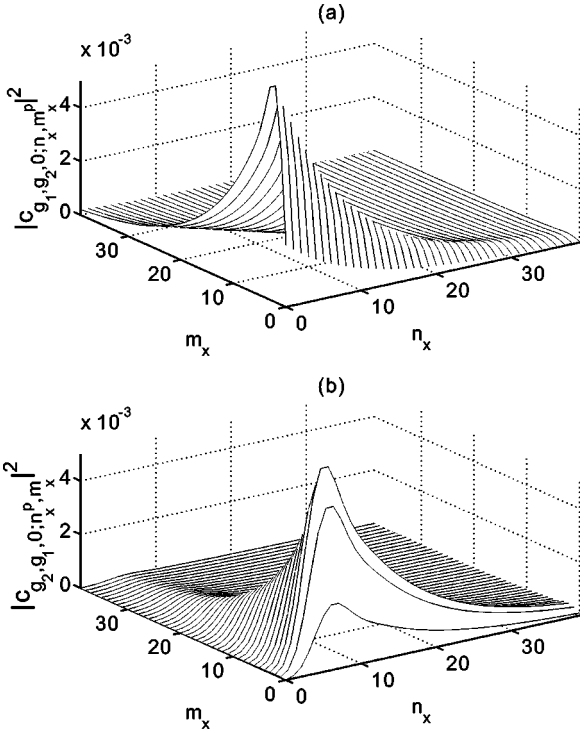

FIG. 8. Motional state distribution before (a) for $|c_{g_1,g_2,0;n_x,m_x^p}(t=0)|^2$ and (b) for $|c_{g_2,g_1,0;n_x^p,m_x}(t=2\pi)|^2$ after the adiabatic passage process.

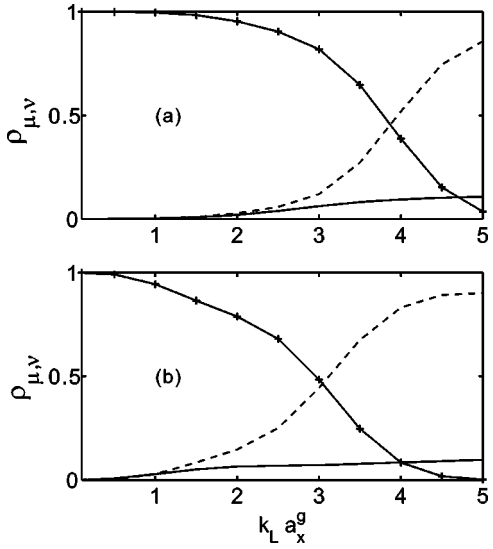

FIG. 9. Results of adiabatic transfer for co-propagating (a) and counterpropagating (b) lasers. The solid lines with crossed ''+'' calculation data points denote fidelity of the swap gate $[\rho_{g_2,g_1}(t=2\pi)]$. The smooth solid lines denote survival probabilities of remaining in the initial state $[\rho_{g_1,g_2}(t=2\pi)]$. The dashed lines denote the excited probabilities; the sum of probabilities over the remaining three electronic states $[\rho_{e,g_2}(t=2\pi)+\rho_{g_2,g_2}(t=2\pi)+\rho_{g_2,e}(t=2\pi)]$. All parameters except $k_L a_x^g$ are the same as in Figs. 7 and 8.

decoherence due to the nearest-neighbor coupling $\mathcal{H}_O^{[2]}$, can be approximately estimated from the combined ME of individual atoms *A* and *B*. We note the single qubit motional decoherence has been studied earlier in Sec. II.

We now present the numerical results for the $|g_1,g_2,0\rangle \rightarrow |g_2,g_1,0\rangle$. Similar to the single qubit case, we performed simulations for several different choices of the two atom initial motional states. We find high transfer fidelities under all conditions when ME on single qubit operations is acceptable. In Figs. 7 and 8, we show selected results for adiabatic passage with $\Omega_1^\mu(t)=\Omega_1^{\mu 0}/\cosh^2(-|t-t_\mu|/\tau_\mu)$. We used $g_\mu=50(\hbar\omega_x^g)$, $\Omega_1^{\mu 0}=100(\hbar\omega_x^g)$, $t_B=\pi$, $\tau_\mu=\pi/15$, and $t_A=t_B+\tau_\mu$ for the counterintuitive pulse sequence [6]. We note the adiabatic passage, convincingly displayed in Fig. 7, works even for $k_1 a_x^g=1$ and for an initial thermal distribution of amplitudes $c_{n_x}(0)$ [see Eq. (21)] with $k_B T/\hbar\omega_x^g=10$. Figure 8 denotes motional state wave-packet distribution before (for atom *A*) and after (for atom *B*) the adiabatic passage. The asymmetric distribution is due to the use of wave-packet basis m_x^p for atom *B* in Fig. 8(a) and n_x^p for atom *A* in Fig. 8(b) as given by Eq. (39). The total time of adiabatic passage is chosen to be one harmonic-oscillation period $t=2\pi(1/\omega_x^g)$ in this simulation. Better results are obtained for higher values of $\Omega_1^{\mu 0}$ and g_μ and shorter pulses (with smaller) τ_μ that minimize ME from the off-diagonal term $\mathcal{H}_O^{[2]}$.

In Fig. 9 we compare the dependence of swap gate fidelity on Lamb-Dicke parameter $k_L a_x^g$. We have used a coherent motional state distribution with $c_{n_x}(0)=\sqrt{\rho_{n_x}^{\rm cm}}$ as from Eq.

(21) with $k_B T/\hbar\omega_x^g = 10$. Even with the wave-packet basis technique, up to 300 motional states are needed for each atom to obtain converged results when $k_L a_x^g = 5$. Our numerical results (Fig. 9) indicate that fidelity of swap is always higher for co-propagating lasers. Physically this is perhaps not so surprising since, for Raman transition in a single three level Λ-type atom, motional effects can completely disappear for co-propagating driving fields. Mathematically, co-propagating field configuration provides higher fidelity of transfer because the coupling of different double triplets of the two atoms are more coherent. This point will be further illustrated elsewhere for adiabatic transfer in Λ-type three level atoms.

Finally we emphasize that the wave-packet structure exists as long as motional states are confined in harmonic traps, i.e., even when trap frequencies become atom dependent and internal state dependent. Our analysis of the dark-state-like structures remains the same.

IV. CONCLUSIONS

In this paper we performed careful investigations of decoherence due to ME for electronic state coded trapped qubits. For single bit operations on harmonically trapped atom or ions mediated by a near resonant plane-wave laser field, by introducing a wave-packet basis in the excited state, we were able to perform considerably cleaner analysis to simplify the ME. We find that a single parameter η measures the achievable fidelity of arbitrary single bit rotations. We also performed numerical calculations, which demonstrated our understanding and provided quantitative limits for experiments; the LDL is always required to maintain a high fidelity for arbitrary single bit rotations with plane-wave laser excitation. With a degenerate Raman configuration using co-propagating pump and Stokes fields, this restriction can be effectively lifted. Our results indicate that a pure motional state is not necessarily preferred, although a qubit with an initial motional ground state does give rise to the highest achievable fidelity. In actual experimental implementations, large values of Ω_L are also needed to assure negligible motional dephasing during τ [24]. Furthermore, due to the periodic revival nature inside harmonic traps, one can always wait for a period $2\pi/\omega_x^g$ for subsequent single bit operations since the motional wave function then rephases to its initial state.

For quantum gate operations involving two trapped qubits, ME can again be studied with our wave-packet technique to yield simplified physical pictures. In particular, we considered the popular quantum information processing scheme of two three level atoms trapped inside a high Q optical cavity [6]. We find that LDL along the transverse direction can be significantly compromised without causing much decoherence for conditional logic gate operations based on the adiabatic passage protocol [6]. This paper will also shed light on devising schemes for overcoming ME decoherence and error corrections in trapped atomic or ionic qubits.

ACKNOWLEDGMENTS

The authors thank Dr. T. Uzer and Dr. M. S. Chapman for their helpful discussions. We also thank Dr. Müstecaplıoğlu for supplying an efficient Fortran subroutine to evaluate $\eta_{n_x m_x}$. This work benefited from our participation of the recent workshop on quantum degenerate gases at the Lorentz Center, University of Leiden. We thank H. Stoof for the hospitality. This work was supported by ONR Grant No. 14-97-1-0633 and ARO/NSA Grant No. G-41-Z05.

[1] P. W. Shor, in *Proceedings of 35th Annual Symposium on the Foundations of Computer Science*, edited by S. Goldwasser (IEEE Computer Society, Los Alamitos, CA, 1994); A. Ekert and R. Jozsa, Rev. Mod. Phys. **68**, 733 (1996).

[2] Q.A. Turchette *et al.*, Phys. Rev. Lett. **81**, 3631 (1998); C. Monroe *et al.*, *ibid.* **75**, 4714 (1995); Q.A. Turchette *et al.*, *ibid.* **75**, 4710 (1995).

[3] D. Boschi *et al.*, Phys. Rev. Lett. **80**, 1121 (1998); Dik Bouwmeester *et al.*, Nature (London) **390**, 575 (1997); A. Furusawa *et al.*, Science **282**, 706 (1998).

[4] Dik Bouwmeester *et al.*, Phys. Rev. Lett. **82**, 1345 (1999).

[5] J.I. Cirac and P. Zoller, Phys. Rev. Lett. **74**, 4091 (1995).

[6] T. Pellizzari *et al.*, Phys. Rev. Lett. **75**, 3788 (1995).

[7] J. Javanainen *et al.*, J. Opt. Soc. Am. B **1**, 111 (1984).

[8] C. Monroe *et al.*, Phys. Rev. Lett. **75**, 4011 (1995); M. Morinaga *et al.*, *ibid.* **83**, 4037 (1999); Ch. Roos *et al.*, *ibid.* **83**, 4713 (1999); E. Peik *et al.*, Phys. Rev. A **60**, 439 (1999).

[9] R. Bonifacio *et al.*, Phys. Rev. A **61**, 053802 (2000); e-print quant-ph/9906115.

[10] J.F. Poyatos *et al.*, Phys. Rev. Lett. **81**, 1322 (1998); A. Sorensen and K. Molmer, *ibid.* **82**, 1971 (1999); K. Molmer and A. Sorensen, *ibid.* **82**, 1835 (1999).

[11] S. Schneider and G.J. Milburn, Phys. Rev. A **59**, 3766 (1999).

[12] T. A. B. Kennedy and P. Zhou (unpublished).

[13] M. Cirone *et al.*, Phys. Rev. A **57**, 1202 (1998).

[14] H.P. Zeng *et al.*, Phys. Rev. A **59**, 2174 (1999).

[15] R.L. de Matos Filho and W. Vogel, Phys. Rev. Lett. **76**, 608 (1996).

[16] L. You *et al.*, Phys. Rev. A **51**, 4712 (1995).

[17] A.C. Doherty, A.S. Parkins, S.M. Tan, and D.F. Walls, J. Opt. B: Quantum Semiclassical Opt. **1**, 475 (1999).

[18] D.J. Wineland and W.M. Itano, Phys. Rev. A **20**, 1521 (1979).

[19] W. Vogel and R.L. de Matos Filho, Phys. Rev. A **52**, 4214 (1995).

[20] G.M. Gorigi *et al.*, Phys. Rev. A **57**, 2909 (1998).

[21] H. Moya-Cessa, A. Vidiella-Barranco, J.A. Roversi, Dagoberto S. Freitas, and S.M. Dutra, Phys. Rev. A **59**, 2518 (1999).

[22] G. Herzberg, *Molecular Spectra and Molecular Structure, I. Spectra of Diatomic Molecules* (Van Nostrand Reinhold Company, New York, 1950).

[23] K.E. Kahill and R.J. Glauber, Phys. Rev. **177**, 1857 (1969).

[24] D.J. Wineland *et al.*, J. Res. Natl. Inst. Stand. Technol. **103**, 259 (1998).
[25] J. Ye *et al.*, Phys. Rev. Lett. **83**, 4987 (1999).
[26] A. Barenco *et al.*, Phys. Rev. A **52**, 3457 (1995).
[27] C.J. Hood, T.W. Lynn, A.C. Doherty, A.S. Parkins, and H.J. Kimble, Science **287**, 1447 (2000); A.C. Doherty, T.W. Lynn, C.J. Hood, and H.J. Kimble, Phys. Rev. A **63**, 013401 (2000).
[28] We thank Dr. M. Chapman for a discussion that clarified the physics picture of this point.